# The eXtended Finited Element Method for frictional contact problem

**Zhiqiang Hu[1,*], Guogang Fan[1], Gao Lin[1]**

[1] Faculty of Infrastructure Engineering, School of Hydraulic Engineering, Dalian University of Technology, No.2 Linggong Road, Ganjingzi District, Dalian, 116024, China
* Corresponding author: huzhq@dlut.edu.cn

**Abstract** Frictional contact is often observed in the problems with the presence of crack surface. In order to take effects of contact of crack surfaces on the structural response, in the framework of mesh-based approaches, e.g. Finite Element Method (FEM) or Boundary Element Method (BEM), usually the contact surfaces need to be discretized and nodes are placed on the contact surfaces, although the meshes for both contact surfaces are not necessary to be matched with each other. However, the crack surface will evolve under loading, so remeshing is needed to make the meshes consistent with the geometry of crack surfaces.

In this paper, we deal with the frictional contact problems resulting from presence of crack surfaces by combining the eXtended Finite Element Method (XFEM) and B-Differential Equation Method (BDEM). XFEM is used to model the discontinuities of displacement fields in the interior of the elements without the need for the remeshing of the domain. In BDEM, the normal and tangential contact conditions are formulated as B-differentiable equations and satisfied accurately. The B-differentiable Newton solution strategy with the good convergence performance is employed to solve with system equations. The Numerical examples including 2D and 3D frictional contact problems are given to demonstrate the effectiveness and accuracy of the presented approach.

**Keywords** Frictional contact, eXtended Finite Element Method, B-differential Equation

## 1. Introduction

Separation, stick and frictional sliding are often observed in the problems with the presence of crack surface or crack propagation. In order to take effects of contact on the behavior of cracks and structure, in the framework of mesh-based approaches, e.g. traditional Finite Element Method (FEM) or Boundary Element Method (BEM), remeshing is needed to trace the crack surfaces and make the meshes consistent with the geometry of crack surfaces. Although the meshes for contact surfaces in the framework of FEM and BEM are not necessary to be matched with each other, remeshing will result in the increase of the computational cost and additional mapping of the computational results from the original meshes to updated meshes. The invention of embedded discontinuity method, in which the discontinuity surfaces can be embedded in the element and traced effectively without remeshing, e.g., eXtended Finite Element Method[1], provides an alternative method to deal with contact problem, especially for the case in which contact surfaces evolve in the structure subjected to the complicated cyclic loads. The key feature of XFEM is that the discontinuity across crack surface can be resolved by additional enrichment functions and additional nodal degrees of freedom.

The contact problem which is solved in the content of XFEM is firstly proposed by J. Dolbow Möes et al. [2]. The contact condition were enforced by penalty method and the LArge Time INcrement method (LATIN) was employed to solve the system equations. Recently, FS. Liu and R.I. Borja [3] proposed the Petrov-Galerkin variational formation for the frictional contact problem, and the augmented Lagrangian technique was used for the enforcement of contact conditions. I. Nistor et al. [4] developed a hybrid X-FEM contact element for frictionless large sliding contact problem, in which the augmented Lagrangian method was also employed.
Due to the good performance and convergence property of B-differentiable Equations method to solve the frictional contact problem, so we extended this method to model the two and

three-dimensional elastic frictional contact problems between the crack surfaces in the framework of XFEM. The structure of the paper is given as follows. Firstly, the variational formulation for frictional contact problem and the contact conditions are reviewed in Section 2. Secondly, the details of computation of discontinuities across contact surfaces and the equivalent nodal force due to the contact force acting at the contact surface are described in the framework of XFEM in Section 3. In Section 4, after the B- differentiable equations method for frictional contact problem is introduced we give the formulation and solution procedure of the combined XFEM and BDEM for frictional contact problem. Two numerical examples are presented in Section 5 for demonstrate the feasibility and accuracy of the proposed method. The concluding remarks are given in the last section.

## 2. Problem formulation

### 2.1. General description of the problem

Consider a body $\Omega \in R^n$, (n=2,3) embedded with two crack surfaces $\Gamma_c^1$ and $\Gamma_c^2$ which are also taken as the contact surfaces. We denote by $\Gamma$ the outside boundary of $\Omega$. $\Gamma$ is composed by $\Gamma_u$ on which prescribed displacements are imposed, $\Gamma_\sigma$ on which prescribed tractions are imposed and the crack surfaces, i.e. $\Gamma=\Gamma_u \cup \Gamma_\sigma \cup \Gamma_c^1 \cup \Gamma_c^2$. The crack surfaces may intersect the boundary $\Gamma$ with points in 2D case or lines in 3D case. In the following sections, the variables with superscripts '1' and '2' indicate that they are related to $\Gamma_c^1$ and $\Gamma_c^2$ respectively. On the two crack surfaces, the displacements and tractions are denoted as $u_c^i, t_c^i (i=1,2)$ respectively. It should be noted that since the contact surfaces are embedded in the element, they are assumed to be coincident initially, i.e., no initial gap exists between the contact surfaces.

The quasi-static loading by a body force $\mathbf{b}_f$ and given traction $\bar{\mathbf{t}}$ on $\Gamma_\sigma$ are assumed. The equilibrium equation and boundary conditions are described as follows.

$$\mathrm{div}(\boldsymbol{\sigma}) + \mathbf{b}_f = 0 \quad \text{in } \Omega \setminus \Gamma_c \tag{1}$$

$$\begin{aligned} &\boldsymbol{\sigma} \cdot \mathbf{n}_\sigma = \bar{\mathbf{t}} && \text{on } \Gamma_\sigma \\ &\mathbf{u} = \bar{\mathbf{u}} && \text{on } \Gamma_u \\ &\boldsymbol{\sigma} \cdot \mathbf{n}_c^1 = \mathbf{t}_c^1 && \text{on } \Gamma_c^1 \\ &\boldsymbol{\sigma} \cdot \mathbf{n}_c^2 = \mathbf{t}_c^2 && \text{on } \Gamma_c^2 \end{aligned} \tag{2}$$

Where, $\boldsymbol{\sigma}$ is the Cauchy stress tensor, $\bar{\mathbf{u}}$ is the prescribed displacement vector on boundary $\Gamma_u$. $\mathbf{n}_\sigma$ is the unit normal vector to the boundary $\Gamma_\sigma$. $\mathbf{n}_c^i$ and $\mathbf{t}_c^i$ (i=1,2) are the unit normal vectors to the contact surface $\Gamma_c^i$ and contact stresses on $\Gamma_c^i$ respectively.

### 2.2. Frictional contact constraint formulation by B-differentiable equation

According to the assumption of small displacement and small strain, a contact pair consists of the two points with the same coordinates on $\Gamma_c^1$ and $\Gamma_c^2$, which are denoted as $\mathbf{x}_c^1$ and $\mathbf{x}_c^2$ respectively. A local coordinate system **nab** is established on $\Gamma_c^2$ as shown in Figure 1. Therein, **n** is the normal vector and **a** and **b** are tangential vectors to the contact surface $\Gamma_c^2$.

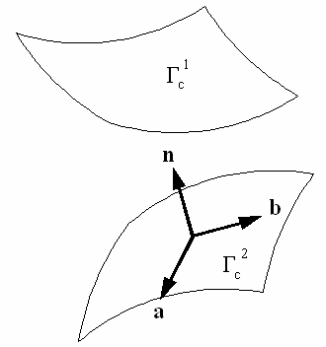


Figure 1. Local coordinate system on the contact surface $\Gamma_c^2$

Then the normal gap $\Delta u_n$ between a contact pair can be defined as

$$\Delta u_n(\mathbf{x}_c) = \left(\mathbf{u}\left(\mathbf{x}_c^1\right) - \mathbf{u}\left(\mathbf{x}_c^2\right)\right)\cdot \mathbf{n} \tag{3}$$

Where, $\mathbf{u}\left(\mathbf{x}_c^1\right)$ and $\mathbf{u}\left(\mathbf{x}_c^2\right)$ are the displacements of contact points on $\Gamma_c^1$ and $\Gamma_c^2$ respectively.

Since part of the system energy will be dissipated due to the friction, the frictional contact problem is nonlinear and path-dependent and increment solution strategy is needed. So at every load step, when frictional sliding takes place between two contact surfaces, relative incremental sliding in tangential directions are defined as follows.

$$\Delta du_a = \left(\mathbf{du}\left(\mathbf{x}_c^1\right) - \mathbf{du}\left(\mathbf{x}_c^2\right)\right)\cdot \mathbf{a} \tag{4a}$$

$$\Delta du_b = \left(\mathbf{du}\left(\mathbf{x}_c^1\right) - \mathbf{du}\left(\mathbf{x}_c^2\right)\right)\cdot \mathbf{b} \tag{4b}$$

Where, **du** is the vector of incremental displacement at current load step.

The contact conditions in normal and tangential directions proposed by Christensen *et al*. [5] are expressed as a B-differentiable equation set. Due to the assumption of small displacement and small strain, the discrete point-to-point contact model is employed in the following, so that the contact conditions will be formulated by the quantities at these discrete contact pairs. For *i*-th contact pair, they are written as

$$\mathrm{H}_2^i\left(\mathbf{du}_c^i, \mathbf{dP}^i\right) = \min\left\{r\Delta u_n^i, P_n^i\right\} = 0 \tag{5a}$$

$$\mathrm{H}_3^i\left(\mathbf{du}_c^i, \mathbf{dP}^i\right) = P_a^i - \lambda P_a^i(r) = 0 \tag{5b}$$

$$\mathrm{H}_4^i\left(\mathbf{du}_c^i, \mathbf{dP}^i\right) = P_b^i - \lambda P_b^i(r) = 0 \tag{5c}$$

Where, $\mathbf{du}_c^i$ is the incremental displacement vector of two contact points consisting of the *i*-th contact pair. $\mathbf{dP}^i$ is the vector of increment contact force acting at the *i*-th contact pair. $P_n^i$, $P_a^i$ and $P_b^i$ are the total contact forces in the normal and two tangential directions. *r* is a positive scalar. $\Delta u_n^i$ is the normal gap. Eq. (5a) corresponds to the normal contact condition, Eqs. (5b) and (5c) correspond to the tangential contact conditions in local *a* and *b* directions respectively. The

definitions of $P_a^i(r)$, $P_b^i(r)$ and $\lambda$ are given as follows.

$$P_a^i(r) = P_a^i - r\Delta du_a^i \tag{6a}$$

$$P_b^i(r) = P_b^i - r\Delta du_b^i \tag{6b}$$

$$\lambda = \min\left\{ \mu \min\left\{P_n^i, 0\right\} \Big/ \sqrt{\left(P_a^i(r)\right)^2 + \left(P_b^i(r)\right)^2}\ , 1 \right\} \tag{7}$$

Where, $\Delta du_a^i$ and $\Delta du_b^i$ are tangential incremental relative displacements in local *a* and *b* directions respectively. The incremental relative displacements in global and local coordinate system for i-th contact pair at current load step are defined as

$$\Delta du_j^i = du_j^{i1} - du_j^{i2} \quad , \quad \left(j = n, a, b \quad or \quad x, y, z\right) \tag{8}$$

The normal relative displacement for i-th contact pair at current load step is defined as

$$\Delta u_n^i = \Delta \overline{u}_n^i + \left(du_n^{i1} - du_n^{i2}\right) \tag{9}$$

Where, $\Delta \overline{u}_n^i$ is the initial normal relative displacements at current load step.

## 3. Discretization by XFEM formulation

The XFEM is a promising method to simulate the existence and growth of the discontinuities, such as cracks, without the need to make the mesh conforming it. In order to characterize the discontinuous displacement field resulted from the embedded discontinuity, the Heaviside functions or asymptotic crack tip functions are often used to enrich standard continuous displacement fields of the elements cut entirely by the discontinuity surface or those including the crack tip in 2D or crack front in 3D case, respectively. The additional nodal degrees of freedom corresponding to these enrichment functions are needed.

### 3.1. The XFEM approximation

In XFEM, the displacement approximation at an arbitrary point **x** in the element with embeded discontinuity takes the form

$$\mathbf{u}(\mathbf{x}) = \overline{\mathbf{u}}(\mathbf{x}) + [\![\mathbf{u}(\mathbf{x})]\!] = \sum_{i=1}^{nd} N_i \overline{\mathbf{u}}_i + \sum_{j=1}^{nd} \mathbf{b}_{Hj} N_j \left(H(\mathbf{x}) - H(\mathbf{x}_j)\right) + \sum_{k=1}^{nd} N_k \sum_{l=1}^{4} \mathbf{c}_{kl} \left(g_l(r,\theta) - g_l(r_k,\theta_k)\right) \tag{10}$$

Where, nd is the number of nodes in one element, $\overline{\mathbf{u}}_i$ is the continuous displacement field at node i. The last two terms form the discontinuous part $[\![\mathbf{u}]\!]$. H(**x**) is generalized Heaviside function, and $\mathbf{b}_{Hj}$ is the vector of additional translational DOFs corresponding to generalized Heaviside function. $g_l$ ($l$=1,2,3,4) are the tip enrichment functions, and $\mathbf{c}_{kl}$ is the vector of additional translational DOFs related to the l-th tip branch function for node k. The generalized Heaviside function is defined as

$$H(\mathbf{x})=\begin{cases}=1 & (\mathbf{x}-\mathbf{x}^*)\cdot\mathbf{n}\geq 0\\ =-1 & (\mathbf{x}-\mathbf{x}^*)\cdot\mathbf{n}<0\end{cases} \tag{11}$$

Where, $\mathbf{x}^*$ is the closest point on the crack surface for point $\mathbf{x}$. The unit normal vector $\mathbf{n}$ is defined in Figure 1. The vector functions $\boldsymbol{g}(r,\theta)$ are defined as

$$\begin{aligned}&\mathbf{g}(r,\theta)=\mathbf{g}(\mathbf{x})=\{g_1(r,\theta),g_2(r,\theta),g_3(r,\theta),g_4(r,\theta)\}\\&=\left\{\sqrt{r}\sin\frac{\theta}{2},\sqrt{r}\cos\frac{\theta}{2},\sqrt{r}\sin\frac{\theta}{2}\sin\theta,\sqrt{r}\cos\frac{\theta}{2}\sin\theta\right\}\end{aligned} \tag{12}$$

Where, $(r,\theta)$ are the local polar coordinates of point $\mathbf{x}$. The local polar coordinate system is established at the crack tip in 2D case [1] or crack front in 3D case [7]. In (12), the first function is discontinuous across the discontinuity surface whereas the other three functions are continuous. So the displacement jump across the discontinuity surface comes from the generalized Heaviside function (11) and the first function in (12).

The equilibrium equations are obtained after the discretization of weak form of equilibrium equations and the implementation of the contact constrain by Lagrangian multiplier method.

$$\mathbf{K}\mathbf{u}=\mathbf{f}+\mathbf{F}_c(\mathbf{P}) \tag{13}$$

Where, $\mathbf{u}$ is the vector of nodal displacements including the conventional DOFs and additional nodal enrichment DOFs. $\mathbf{K}$ is the stiffness matrix. $\mathbf{f}$ is the nodal load vector resulted from body force and prescribed traction on $\Gamma_\sigma$. $\mathbf{F}_c$ is the equivalent nodal force vector resulted from the contact forces $\mathbf{P}$ acting on the contact surfaces which are equivalent to the contact stress acting on the crack surface. Note that the unknown vectors in Eq.(13) are $\mathbf{u}$ and $\mathbf{P}$.

### 3.2. The derivation of equivalent nodal force resulted from the contact forces on the crack surfaces in the XFEM formulation

In the case that the contact surfaces are embedded in the interior of element, the contact pairs can be easily formed at the positions where the crack line/surface intersects the edges of the element. The two contact points in one contact pair have the same coordinates as the intersection point. Let $\mathbf{x}_c$ be the position of any contact pair. Then the displacement jump can be computed according to (10)~(12) and obtained as

$$[[\mathbf{u}(\mathbf{x}_c)]]=\mathbf{u}(\mathbf{x}_c^1)-\mathbf{u}(\mathbf{x}_c^2)=2\sum_{j=1}^{nd}\mathbf{b}_{Hj}N_j(\mathbf{x}_c)+2\sqrt{r}\sum_{k=1}^{nd}N_k(\mathbf{x}_c)\mathbf{c}_{k1} \tag{14}$$

Where, $\mathbf{x}_c^1$ and $\mathbf{x}_c^2$ are two contact points in the contact pair located on crack surface $\Gamma_c^1$ and $\Gamma_c^2$ respectively. Because no initial gap exists between the two contact surfaces, $\mathbf{x}_c^1=\mathbf{x}_c^1=\mathbf{x}_c$.

The equivalent nodal forces $\mathbf{F}_c$ can be obtained from virtual work done by the contact forces $\mathbf{P}$ acting at the contact points. It is assumed that the element is cut by contact surface into two pieces, as shown in Figure 2. In order to clarify the following procedure for more general cases, the nodes

are assumed to be enriched by both the generalized Heaviside and branch functions. In Figure 2, we focus on the contact pair $i_1$ on the edge "s", and the two contact points belonging to the $\Gamma_c^1$ and $\Gamma_c^2$ are denoted as $i_1^1$ and $i_1^2$ respectively. For every contact pair, the contact force acting at the point $i_1^1$ denoted by vector $\mathbf{P}^{i_1}$ is used to represent the pair of contact forces.

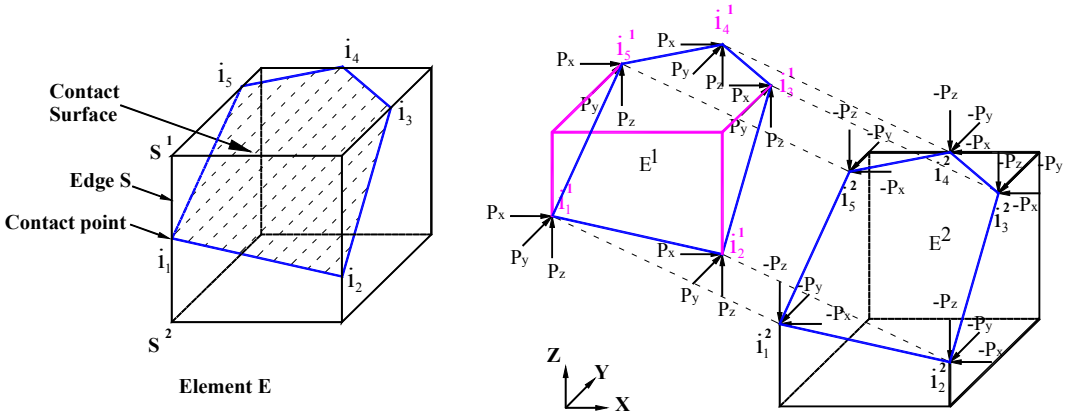


Figure 2 The element cut by contact surface and the contact forces

Then using (14), the virtual work done by the contact force at the contact pair $i_1$ is

$$W_{i_1} = \delta\mathbf{u}\left(\mathbf{x}_c^1\right)\cdot\mathbf{P}^{i_1} + \delta\mathbf{u}\left(\mathbf{x}_c^2\right)\cdot\left(-\mathbf{P}^{i_1}\right) = \delta\left[\left[\mathbf{u}\left(\mathbf{x}_c\right)\right]\right]\cdot\mathbf{P}^{i_1} = 2\left(\sum_{j=1}^{nd}\delta\mathbf{b}_j N_j\left(\mathbf{x}_c\right) + \sqrt{r}\sum_{k=1}^{nd} N_k\left(\mathbf{x}_c\right)\delta\mathbf{c}_{k1}\right)\cdot\mathbf{P}^{i_1} \quad (15)$$

As the contact pairs locate on the edges of element, so only the two shape functions related to nodes on the edge are nonzero. For example, in Figure 2, $\mathbf{x}_c$ locate on the edge "s", therefore only the shape function of nodes $s^1$ and $s^2$ may take nonzero values. The virtual work is then transformed into

$$\begin{aligned} W_{i_1} &= \left(2\left(\delta\mathbf{b}_{s^1}N_{s^1}\left(\mathbf{x}_c\right) + \delta\mathbf{b}_{s^2}N_{s^2}\left(\mathbf{x}_c\right)\right) + 2\sqrt{r}\left(N_{s^1}\left(\mathbf{x}_c\right)\delta\mathbf{c}_{s^1 1} + N_{s^2}\left(\mathbf{x}_c\right)\delta\mathbf{c}_{s^2 1}\right)\right)\cdot\mathbf{P}^{i_1} \\ &= \left\{\delta\mathbf{b}_{s^1}, \delta\mathbf{b}_{s^2}, \delta\mathbf{c}_{s^1}, \delta\mathbf{c}_{s^2}\right\}\cdot\left\{2N_{s^1}\mathbf{P}^{i_1}, 2N_{s^2}\mathbf{P}^{i_1}, 2\sqrt{r}N_{s^1}\mathbf{P}^{i_1}, 2\sqrt{r}N_{s^2}\mathbf{P}^{i_1}\right\}^T = \left(\delta\mathbf{u}^{add}\right)^T\cdot\mathbf{F}_c^{i_1} \end{aligned} \quad (16)$$

Where,

$$\begin{aligned} \delta\mathbf{u}^{add} &= \left\{\delta\mathbf{b}_{s^1}, \delta\mathbf{b}_{s^2}, \delta\mathbf{c}_{s^1}, \delta\mathbf{c}_{s^2}\right\}^T \\ \mathbf{F}_c^{i_1} &= \left\{2N_{s^1}\left(\mathbf{x}_c\right)\mathbf{P}^{i_1}, 2N_{s^2}\left(\mathbf{x}_c\right)\mathbf{P}^{i_1}, 2\sqrt{r}N_{s^1}\left(\mathbf{x}_c\right)\mathbf{P}^{i_1}, 2\sqrt{r}N_{s^2}\left(\mathbf{x}_c\right)\mathbf{P}^{i_1}\right\}^T \end{aligned} \quad (17)$$

$\mathbf{F}_c^{i_1}$ is the equivalent nodal loads resulted from the contact forces $\mathbf{P}^{i_1}$ acting at the contact pair $i_1$ on the embedded contact surfaces in one element. Thus the total nodal loads $\mathbf{F}_c$ resulted from the contact forces can be obtained by assembling $\mathbf{F}_c^{i_1}$ for every contact pair $i_1$.

## 4. Solution procedure

The equilibrium equation (13) and the contact equations (5) lead to the system equations which have the forms

$$\begin{aligned}
\mathbf{H}_1 &= \mathbf{Ku} - \mathbf{f} - \mathbf{F}_c(\mathbf{P}) = \mathbf{0} \\
\mathbf{H}_2 &= \left\{\mathrm{H}_2^1, \mathrm{H}_2^2, \mathrm{K}, \mathrm{H}_2^{NC}\right\}^T = \mathbf{0} \\
\mathbf{H}_3 &= \left\{\mathrm{H}_3^1, \mathrm{H}_3^2, \mathrm{K}, \mathrm{H}_3^{NC}\right\}^T = \mathbf{0} \\
\mathbf{H}_4 &= \left\{\mathrm{H}_4^1, \mathrm{H}_4^2, \mathrm{K}, \mathrm{H}_4^{NC}\right\}^T = \mathbf{0}
\end{aligned} \tag{18}$$

Where, NC is the total number of contact pairs. The unknown vectors of displacement **du** and contact forces **dP** in the form of increment are grouped and denoted by vector **z**, i.e., $\mathbf{z}=\{\mathbf{du}, \mathbf{dP}\}^T$. The second to fourth equations in Eq. (18) are B-differentiable equations, because "min" operator in (5) is B-differentiable[5].

Because of the nonlinearity and non-smooth properties of (18), an iterative B-differentiable Newton method [6] which is an extension of classical Newton method, is employed for solving the system equations (18).

## 5. Numerical examples

### 5.1. 2D square plate with a crack

A square plate with 20 ×20m including a center crack oriented at 45° relative to the horizontal is considered. In order to examine the accuracy of the proposed method, two different discretizations by quadrilateral finite elements, which denoted as Model I and Model II respectively, are constructed as shown in Figure 3. In the Model I, the mesh is uniform and the crack intersects the elements at the two adjacent sides. In the Model II, the crack intersects the elements at the two opposite sides. The material is elastic with the properties: Young's Modulus 10GPa, Poisson's ratio 0.3. The bottom boundary of the plate is fixed. At the top boundary, uniform displacements with the value of -0.1m in vertical direction are prescribed. In this example, we assume that the crack surface can slide but the crack tip will not advance. The different friction coefficients with 0.1, 0.8 and 1.2 are used to test the convergence of the proposed method.

The results show that the convergent solutions can be obtained for the three frictional coefficients. The total reaction forces at the top boundary for different frictional coefficients are given in Table 1. And the contours of displacement in the case of frictional coefficient 0.1 for the two different discretizations are shown in Figure 4. Table 1 shows that for the two different discretizations, the resultant reaction forces agree well with each other for different frictional coefficients. The Figure 4 shows that the distribution and magnitude of displacements in x and y direction are almost the identical for both models.

Table 1 Resultant of reaction force on the top boundary (Unit: N)

| Model | μ=0.1 | μ=0.8 | μ=1.2 |
|---|---|---|---|
| Mesh I | 973.3 | 1107.4 | 1137.5 |
| Mesh II | 973.7 | 1108.8 | 1141.6 |
| Relative Error | 4.11e-4 | 1.3e-3 | 3.6e-3 |

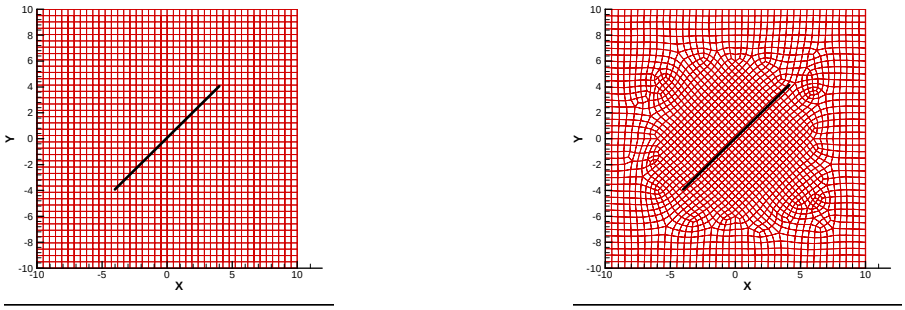

(a) Uniform mesh (Mesh I) (b) Non-uniform mesh (Mesh II)

Figure 3 Two finite element discretizations of the square plate

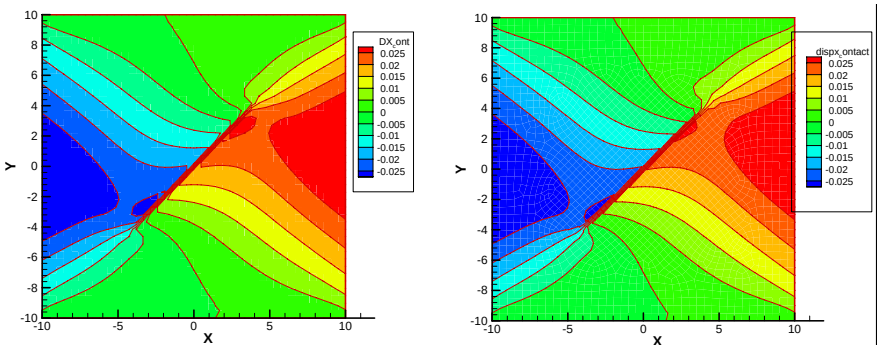

(a) $u_x$(Model I) (b) $u_x$(Model II)

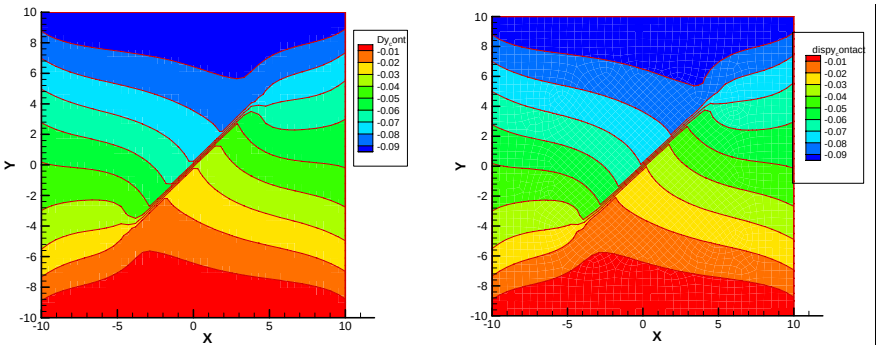

(c) $u_y$ (Model I) (d) $u_y$ (Model II)

Figure 4 Distribution of displacement in the square plate for frictional coefficient 0.1(Unit: m)

### 5.2. Frictional contact of two parts of a 3D beam

In this example, a beam is divided into two identical parts by a contact surface shown in Figure 5. In order of comparison and validation, two finite element models denoted by Model I and Model II are constructed. In Model I the contact surfaces are embedded in the elements, while in Model II the contact surfaces coincide with the element boundaries. The finite element discretizations for the two models are given in Figure 6. The presented method in the framework of XFEM is used for solving Model I and the standard FEM with B-differential equation method for Model II. The material is elastic with the properties: Young's Modulus 1e10Pa, Poisson's ratio 0.3, frictional coefficient 0.1. At the left end of beams, part of the surface, i.e. the shadow area as shown in Figure 6, is fixed. So there are no constraints at the intersection line between contact surfaces and the boundary surfaces

of the cantilever beam. The distribution line load in negative X, Y and Z directions with the same density of 1e5N/m are applied at the top of free end as shown in Figure 6.

In the Model I and Model II, there are 7 nodes at the top of free end denoted by $P_1$ to $P_7$. The displacements at these nodes for the two models are listed in Table 2. It can be seen from this table that the displacements of selected points for both models agree well with each other.

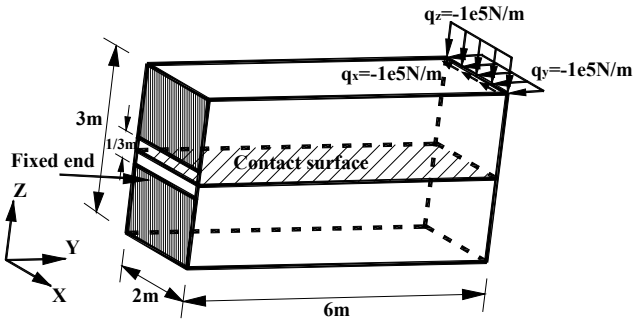


Figure 5 Cantilever beam with the planar crack surface

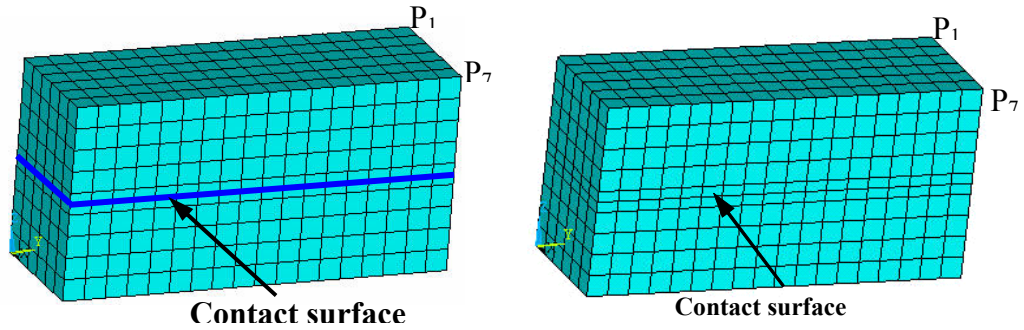


(a) Model I (b) Model II

Figure 6 Two finite element discretizations for the cantilever beam

Table 2 Displacements of nodes at the top of free end (Unit: cm)

| Direction\Model | | Points | | | | | | |
|---|---|---|---|---|---|---|---|---|
| | | $P_1$ | $P_2$ | $P_3$ | $P_4$ | $P_5$ | $P_6$ | $P_7$ |
| X | Model I | -1.782853 | -1.764749 | -1.750595 | -1.744385 | -1.743544 | -1.746958 | -1.745677 |
| | Model II | -1.782816 | -1.764712 | -1.750557 | -1.744346 | -1.743506 | -1.746919 | -1.745638 |
| | **Error** | **2.1e-5** | **2.1e-5** | **2.17e-5** | **2.24e-5** | **2.18e-5** | **2.23e-5** | **2.23e-5** |
| Y | Model I | -0.2448591 | -0.0981012 | 0.0265221 | 0.1475015 | 0.2680483 | 0.3910484 | 0.5294690 |
| | Model II | -0.2450343 | -0.0982756 | 0.0263494 | 0.1473310 | 0.2678800 | 0.3908819 | 0.5293037 |
| | **Error** | **7.16e-4** | **1.78e-3** | **6.51e-3** | **1.16e-3** | **6.28e-4** | **4.26e-7** | **3.12e-4** |
| Z | Model I | -1.517652 | -1.460974 | -1.424242 | -1.389137 | -1.354119 | -1.318229 | -1.269198 |
| | Model II | -1.516629 | -1.459982 | -1.423281 | -1.388208 | -1.353223 | -1.317365 | -1.268366 |
| | **Error** | **6.74e-4** | **6.78e-4** | **6.75e-4** | **6.69e-4** | **6.62e-4** | **6.55e-4** | **6.56e-4** |

## 6. Conclusions

In this paper, a combined eXtend Finite Element method and B-differentiable equations method for solving contact problems in which the contact surfaces are embedded in the elements. There are some salient features for the presented methods. Firstly, in the framework of XFEM, it is very convenient to construct the finite element meshes with minor consideration of the position of crack or contact surfaces. Due to the assumption of small deformation, the contact pairs are easily defined at the intersection points between the contact surfaces and the edges of elements. Secondly, the contact conditions are formulated as B-differentiable equations by the quantities at the contact pairs and satisfied exactly. Thirdly, the B-differential Newton method with guaranteed convergence property is utilized to solve the system equations consisting of equilibrium equations and contact conditions. The 2D and 3D frictional contact examples show the high accuracy and good convergence property of the presented method.

**Acknowledgements**

The first author greatly appreciates the financial support of State Scholarship fund provided by Chinese Scholarship Council and Professor Ted Belytschko to offer him a visiting scholarship position in Northwestern University. He also thanks postdoctors Qinglin Duan, Jeong-Hoon Song, Thomas Menouillard at Northwestern University, Dr. Fushen Liu at Stanford University for their kindly help in studying the XFEM and constructive discussion and suggestions. The support of the China National Science Foundation under grant 51178069 is gratefully acknowledged.

**References**

[1] N. Möes, J. Dolbow, T. Belytschko, A finite element method for crack growth without remeshing. International Journal for Numerical Methods in Engineering, 46 (1999) 131–150.

[2] J. Dolbow, N. Möes, T. Belytschko, An extended finite element method for modeling crack growth with frictional contact, Computer Methods in Applied Mechanics and Engineering, 190 (2001) 6825–6846.

[3] F.S. Liu, R. I. Borja, A contact algorithm for frictional crack propagation with the extended finite element method, International Journal for Numerical Methods in Engineering, 76 (2008) 1489–1512.

[4] I. Nistor, M. L. E. Guiton, P. Massin, N. Möes, S. Géniaut, An X-FEM approach for large sliding contact along discontinuities, International Journal for Numerical Methods in Engineering, 78 (2009) 1407–1431.

[5] P. Christensen, A. Klarbring, J.S. Pang, N. Stromberg, Formulation and comparison of algorithms for frictional contact problems, International Journal for Numerical Methods in Engineering, 42(1998), 145-173

[6] J.S. Pang, Newton's method for B-differentiable equations, Mathematics of Operations Research, (15) 1990 311-341 14.

[7] N. Sukumar, N. Möes, B. Moran, T. Belytschko, Extended finite element method for three-dimensional crack modeling, International Journal for Numerical Methods in Engineering, 48 (2000) 1549-1570